



Discover Generics

Cost-Effective CT & MRI Contrast Agents

 FRESENIUS
KABI

[VIEW CATALOG](#)

AJNR

This information is current as
of September 13, 2025.

Sodium MRI at 7T for Early Response Evaluation of Intracranial Tumors following Stereotactic Radiotherapy Using the CyberKnife

L. Huang, J. Bai, R. Zong, J. Zhou, Z. Zuo, X. Chai, Z.
Wang, J. An, Y. Zhuo, F. Boada, X. Yu, Z. Ling, B. Qu, L.
Pan and Z. Zhang

AJNR Am J Neuroradiol 2022, 43 (2) 181-187

doi: <https://doi.org/10.3174/ajnr.A7404>

<http://www.ajnr.org/content/43/2/181>

Sodium MRI at 7T for Early Response Evaluation of Intracranial Tumors following Stereotactic Radiotherapy Using the CyberKnife

 L. Huang,  J. Bai,  R. Zong,  J. Zhou,  Z. Zuo,  X. Chai,  Z. Wang,  J. An,  Y. Zhuo,  F. Boada,  X. Yu,  Z. Ling,  B. Qu,  L. Pan, and  Z. Zhang



ABSTRACT

BACKGROUND AND PURPOSE: Conventionally, early treatment response to stereotactic radiotherapy in intracranial tumors is often determined by structural MR imaging. Tissue sodium concentration is altered by cellular integrity and energy status in cells. In this study, we aimed to investigate the feasibility of sodium MR imaging at 7T for the preliminary evaluation of radiotherapeutic efficacy for intracranial tumors.

MATERIALS AND METHODS: Data were collected from 16 patients (12 men and 4 women, 24–75 years of age) with 22 intracranial tumors who were treated with stereotactic radiation therapy using CyberKnife at our institution between December 1, 2016, and August 15, 2019. Sodium MR imaging was performed at 7T before and 48 hours, 1 week, and 1 month after CyberKnife radiation therapy. Tissue sodium concentration (TSC) was calculated and analyzed based on manually labeled regions of tumors.

RESULTS: Ultra-high-field sodium MR imaging clearly showed the intratumoral signal, which is significantly higher than that of normal tissue ($t = 5.250$, $P < .001$), but the edema zone has some influence. The average TSC ratios of tumor to CSF in the 22 tumors, contralateral normal tissues, edema zones, frontal cortex, and frontal white matter were 0.66 (range, 0.23–1.5), 0.30 (range, 0.15–0.43), 0.58 (range, 0.25–1.21), 0.25 (range, 0.17–0.42), and 0.30 (range, 0.19–0.49), respectively. A total of 12 tumors in 8 patients were scanned at 48 hours, 1 week, and 1 month after treatment. The average TSC at 48 hours after treatment was 0.06 higher than that before treatment and began to decrease at 1 week. The TSC ratios of 10 continued to decline and 2 tumors increased at 1 month, respectively. Tumor volume decreased by 2.4%–99% after 3 months.

CONCLUSIONS: Changes in the TSC can be quantified by sodium MR imaging at 7T and used to detect radiobiologic alterations in intracranial tumors at early time points after CyberKnife radiation therapy.

ABBREVIATIONS: ATPase = adenosine triphosphatase; CK = CyberKnife; SRT = stereotactic radiotherapy; TSC = tissue sodium concentration; VEGF = vascular endothelial growth factor

Stereotactic radiation therapy (SRT) is an established and effective treatment for intracranial tumors. This therapy consists of a single or a few administrations of high-dose radiation therapy to well-defined tumor targets, rather than repeat low-dose irradiation of tumor cells and normal cells. CyberKnife (CK; Accuray) is a compact, image-guided linear accelerator with a robotic manipulator that is designed for stereotactic radiosurgery

and SRT.¹ Several studies have suggested that radiosurgery may induce apoptotic tumor cell death.^{2–4} The specific cellular changes induced by dose fractionation involving a single or a few high-dose treatments remain unclear. An adequate imaging response of brain tumors after CK involves stable or reduced tumor volumes on serial conventional imaging. However, the biologic changes of the internal environment and cytologic levels of the tumor occur earlier than the visible volume changes after

Received May 8, 2021; accepted after revision November 5.

From the Departments of Neurosurgery (L.H., R.Z., J.Z., X.Y., Z.L., L.P.) and Radiation Oncology (J.B., B.Q.), The First Medical Center of PLA General Hospital, Beijing, China; Department of Neurosurgery (L.H.), The Hospital of 81st Group Army PLA, Zhangjiakou, China; State Key Laboratory of Brain and Cognitive Science (Z. Zou, X.C., Z.W., Y. Z., Z. Zhang.), Institute of Biophysics, Chinese Academy of Sciences, Beijing, China; University of Chinese Academy of Sciences (Z. Zou, X.C., Z.W., Y. Z., Z. Zhang.), Beijing, China; CAS Center for Excellence in Brain Science and Intelligence Technology (Z. Zou, X.C., Z.W., Y. Z., Z. Zhang.), Chinese Academy of Sciences, Beijing, China; Siemens Shenzhen Magnetic Resonance Ltd (J.A.), Shenzhen, China; and Department of Radiology (F.B.), Center for Advanced Imaging Innovation and Research, New York University Grossman School of Medicine, New York, New York.

This work was supported by the National Natural Science Foundation of China (82001804, 31730039), the Ministry of Science and Technology of China grant (2019YFA0707103), and the Chinese Academy of Sciences grants (XDB32010300, ZDBS-LY-SM028).

Please address correspondence to Longsheng Pan, MD, Department of Neurosurgery, The First Medical Center of PLA General Hospital, Fuxing Rd Yard 28, Beijing 100853, China; e-mail: panls301@163.com

 Indicates open access to non-subscribers at www.ajnr.org

 Indicates article with online supplemental data.

<http://dx.doi.org/10.3174/ajnr.A7404>

Signal intensity of ROIs in sodium images

| | Untreated | 48 Hours | 1 Week | 1 Month |
|--------------|------------------|------------------|------------------|------------------|
| Tumor (mean) | 22.85 (SD, 2.61) | 24.19 (SD, 2.45) | 22.28 (SD, 0.27) | 36.08 (SD, 0.12) |
| CSF (mean) | 23.23 (SD, 7.56) | 24.43 (SD, 2.66) | 27.53 (SD, 0.33) | 25.92 (SD, 0.26) |
| Ratio | 0.98 | 0.99 | 0.80 | 1.39 |

radiation therapy. Conventional MR imaging can only show volumetric changes, so there is a lag effect. Thus, increasing numbers of studies are trying to find specific biomarkers of brain tumors for early prediction of therapeutic effects.⁵⁻¹⁰

The biologic parameters of tumor cells, such as acid-base and ionic balance, are different from those of normal cells before treatment⁹ and after radiation therapy¹¹ and chemotherapy.¹² Sodium is the second most abundant MR imaging-active nucleus in the human body, and sodium concentration is sensitive to disease because it is an indicator of cellular and metabolic integrity and ion homeostasis.^{13,14} The cellular process of the sodium ion ($^{23}\text{Na}^+$) homeostasis proceeds via coupled exchange with the potassium ions (K^+) between the intra- and extracellular spaces using the Na^+/K^+ -adenosine triphosphatase (ATPase) enzyme.¹⁵ Dysregulation of the Na^+/K^+ -ATPase or impairment of ATPase-dependent processes causes loss of Na^+ homeostasis and, therefore, increased intracellular sodium concentration, ultimately leading to cell death.¹⁶ Therefore, the Na^+ ion concentration is very sensitive to changes of the tissue metabolic state and cell membrane integrity. Since 1983, sodium MR imaging has been used to detect the Na^+ ions present at different concentrations in various tissues.¹⁷ However, because this technique has a low signal-to-noise ratio and spatial resolution and the imaging time is long, the related research is limited. With the continuous development of MR imaging equipment and technology, the imaging quality of Na^+ continues to improve.

Previous studies have found that the tissue sodium concentration (TSC) is higher than that in normal tissue in patients with diseases such as brain tumors,⁸ stroke,¹⁸ multiple sclerosis,¹⁹ and Huntington disease.²⁰ In 2006, Schepkin et al²¹ detected the early cellular changes of cytotoxic therapy using sodium and proton diffusion MR imaging. They observed that the ADC value and the early TSC increase occurred before the volume change and showed a linear relationship.²¹ This finding suggests that these noninvasive imaging patterns can be used as predictive biomarkers of tumor treatment response. There have been few reports on the application of sodium MR imaging to the evaluation of radiation therapy, and there are no relevant reports evaluating the effects of SRT with CK. Huang et al²² published a case report about this method in 2018. Nevertheless, sodium MR imaging may be a useful noninvasive biomarker for evaluating the early tumor response to therapy, allowing timely adjustment of individualized treatment plans. The goal of the present study was to use sodium MR imaging to noninvasively quantify total TSC and to test whether TSC is altered in intracranial tumors.

MATERIALS AND METHODS

Patient and Tumor Characteristics

We enrolled 16 patients with a total of 22 tumors diagnosed as intracranial tumors by imaging diagnosis or pathology who

underwent SRT with CK from December 1, 2016, to August 15, 2019, at our hospital. Twelve patients were men (75%) and 4 were women (25%), and they had a median age of 52.4 years (range, 24–75 years) at the time of initial CK therapy. The tumors were numbered between 1 and 16 (ie, 1–3, 4.1, 4.2, 5, 6.1, 6.2, 7, 8, 9.1, 9.2, 9.3, 10–14, 15.1, 15.2, 15.3, and 16). Written informed consent was obtained from each participant before study inclusion, and the study was approved by the institutional review board of PLA General Hospital (No. S2018-119-01). All the patients' other treatments followed the principles of primary disease treatment. More patient details are described in the Online Supplemental Data. The patients underwent pretreatment sodium and proton MR imaging scans at a human 7T MR research system (Siemens Healthcare, Erlangen, Germany) and were then treated with SRT using CK. In total, 8 patients (who had a total of 12 tumors) completed follow-up scans at 48 hours, 1 week, and 1 month after treatment.

Quantitative Sodium MR Imaging

Sodium and proton imaging was performed on a human 7T MR research system (Siemens Healthcare, Erlangen, Germany). Proton imaging was first conducted with a 32-channel head coil (Nova Medical Head Coil 1TX/32RX). B_0 shimming parameters were recorded for subsequent shimming during the sodium imaging. Structural and diffusion images were acquired according to the protocols in the Table. Sodium MR imaging was acquired with a homemade birdcage coil. Sodium images with TEs of 0.30 and 2.32 ms were acquired using the twisted projection imaging sequence²³ with the following parameters: FOV = $224 \times 224 \times 224 \text{ mm}^3$, resolution = $3.5 \times 3.5 \times 3.5 \text{ mm}^3$, TR = 174 ms, flip angle = 90° , and acquisition time = 12 minutes 53 seconds.

The sodium images with different TEs were postprocessed to correct for B_0 bias.²⁴ The TSC maps were linearly corrected with reference to tube phantoms with known sodium concentrations of 30, 60, 90, and 120 mM.²⁴ The ROIs for analysis were manually defined on the sodium images by a neurosurgeon. The ratios of the TSC signal between different tissues and CSF were calculated and compared.

ROI Analysis

The ROI analysis was performed in MRICron (<https://www.nitrc.org/projects/mricron>). The tumor ROI was manually defined as a sphere with a radius of 2 mm. The maximum, minimum, and average signal intensities of the ROI were obtained, and the average was selected as the final value. The corresponding information about CSF, contralateral normal tissue, gray matter, and white matter of the frontal cortex was measured by the same method. To reduce error, we used the ratio of TSC values between the ROI and CSF to assess the differences among scans.

Statistical Analysis

We used SPSS 22.0 (IBM) for statistical analyses, using paired *t* tests to analyze the differences in TSC before and after treatment and between different tumors and tissues. $P < .05$ was considered significant. Routine contrast-enhanced MR imaging was performed after

3 months of treatment, and the rate of change in tumor volume before and after treatment was calculated. Tumor dimensions were measured using the Coniglobus formula: $V = 1/6\pi \times a$ (diameter length) $\times b$ (diameter width) $\times m$ (section thickness) $\times c$ (section number).²⁵

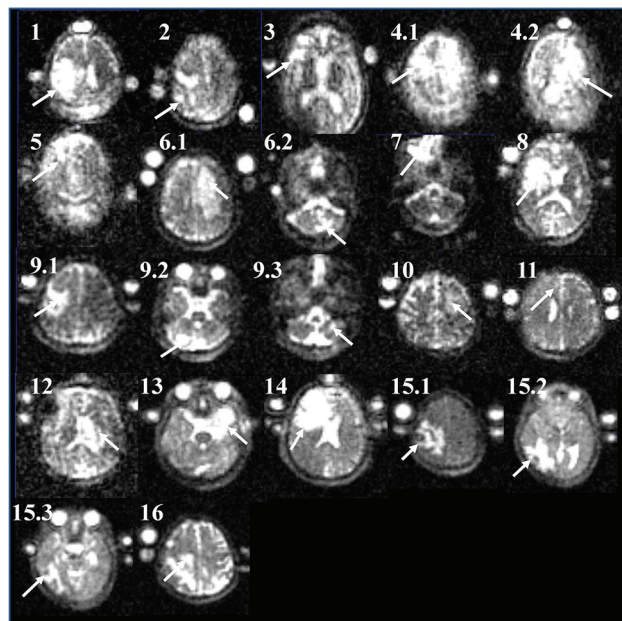


FIG 1. Sodium MR images after B_0 correction of 22 tumors. The arrows pointed to the positions of tumors.

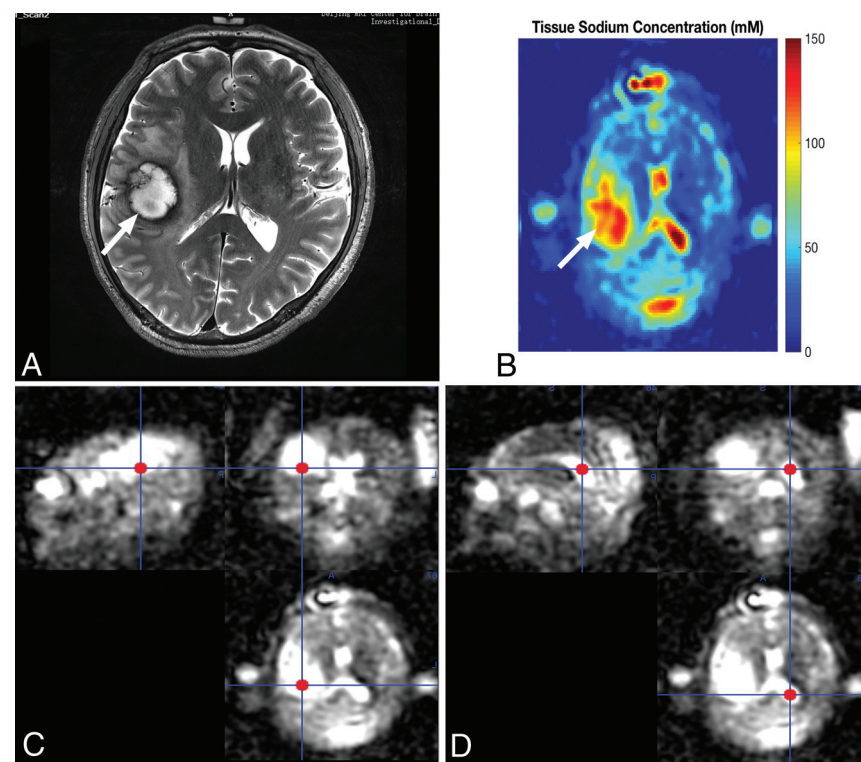


FIG 2. Proton and sodium MR imaging of tumor 1 at 7T. A, Axial T2-weighted image shows brain metastasis of rectal cancer at the right frontal-parietal lobe. B, The reconstructed sodium image. C and D, The ROI of the tumor and CSF in MRIcron software with the quantitative result.

RESULTS

The target irradiation dose to the ROI was 18–22.5 Gy, and the isodose line was 70%–75%, which was completed in 3 fractions. Ultra-high-field sodium MR imaging after B_0 correction clearly showed the intratumoral signal, which is higher than that of normal tissue, but the edema zone has some influence (Fig 1). The uncorrected images can be found in the Online Supplemental Figure. Figure 2 shows the imaging of tumor 1 and the TSC quantitative method. The average TSC ratios between tumor and CSF in the 22 tumors, the contralateral normal tissues, edema zones, frontal cortex, and frontal white matter were 0.66 (range, 0.23–1.5), 0.30 (range, 0.15–0.43), 0.58 (range, 0.25–1.21), 0.25 (range, 0.17–0.40), and 0.30 (range, 0.19–0.49), respectively. The TSC in the tumor before treatment was higher than that in normal tissue ($t = 5.934$, $P < .01$), and the TSC of cortical white matter was higher than that of gray matter ($t = 5.243$, $P < .01$). Although the average TSC in tumors was higher than that in edema zones, there was no significant difference ($t = 1.694$, $P = .10$).

Figure 3 shows the quantitative results of the 22 tumors. The TSC results in different tumors show that brain metastases of liver cancer were the most frequent tumor type in this study. Tumor volume decreased by 2.4%–99% at 3 months after treatment. The TSC values measured in the 12 tumors at 48 hours after treatment were higher than those before treatment by a mean of 0.06. The TSC values of tumors increased by varying degrees at 48 hours after CK treatment and decreased after 1 week. After 1 month, the TSC values continued to decline in 10 tumors, but increased in 2 tumors.

Tumor volume decreased by 2.4%–99% after 3 months. Two tumors showed a second peak in TSC after 1 month and relapsed at 6 and 12 months after treatment. Figure 4 shows a typical case (tumor 14), for which sodium MR imaging signal intensity is listed in the Table.

DISCUSSION

Currently, SRT is used as the main initial treatment for some intracranial tumors, and it can also be used as an adjuvant treatment for postoperative residue or recurrence. The traditional method of evaluating radiotherapeutic efficacy is to observe changes of tumor size using CT/MR imaging after 3 months. However, that method has the disadvantages of the hysteresis effect and the impossibility of observing changes in the intracellular environment of the tumor. Thus, an increasing number of researchers have been exploring noninvasive and quantifiable methods of detecting changes of the intracellular environment after radiation therapy. Sodium MR imaging has mostly been

investigated in intracranial tumors before tumor treatment. For example, Ouwerkerk et al⁹ used hydrogen and sodium MR imaging to quantify the differences in the sodium concentration between normal brain tissue and tumor tissue in 2003. However, studies of sodium MR imaging scans acquired at multiple time points before and after radiation therapy have not been reported. In this study, a good signal-to-noise ratio was obtained under 7T field intensity, and the image quality was satisfactory.

We now discuss environmental changes in tumors. Malignant tumors are characterized by angiogenesis and cell proliferation. This unregulated cell division, which leads to tumor growth, can result from changes in Na⁺/K⁺-ATPase exchange kinetics and increased intracellular sodium concentration,²⁶ accompanied by tumor deterioration.²⁷ Similarly, the increase of tumor neovascularization and interstitial space increases the extracellular volume fraction, which is also related to the potential of the tumor.²⁸ As a result, TSC levels are increased in malignant tumor tissues. The sodium MR imaging data of 22 tumors in 16 patients before

treatment were analyzed and compared. The TSC of the 22 tumors was 55% higher than that of the contralateral normal brain tissue. This result is similar to those of the quantitative analysis of 20 cases of gliomas by Ouwerkerk et al,⁹ who found that the TSC in the tumor and surrounding tissues was 50%–60% higher than that on the contralateral side. In this study, the TSC values in tumors were generally higher than those in edema zones and contralateral normal tissues, while the TSC values in the white matter were higher than those in the gray matter. The TSC values of tumors and edema zones were significantly different from those of normal tissue. Previous studies have also found increased sodium signal intensity in tumors of mice,²⁹ rats,³⁰ and human brains.³¹

Our results showed increased TSC values in additional tumor types, such as metastases, lymphomas, and meningiomas. There is not very good differentiation between the TSC increases in tumors and edema zones. Although the average TSC of tumor tissue in this study was higher than that in edema zones, there was no significant difference. The edema zones surrounding 7 tumors (27.2%) had higher signal values than the tumors.

The pathologic result of the tumors was lung adenocarcinoma. Brain metastases tend to produce vasogenic edema, which is caused by the accumulation of protein-rich fluids in the extracellular space after the blood-brain barrier is destroyed. The increased volume of extracellular space increases the extracellular volume fraction, which also results in an increased TSC value in the edema zone.

The tumor's mechanism of destruction of the blood-brain barrier has 2

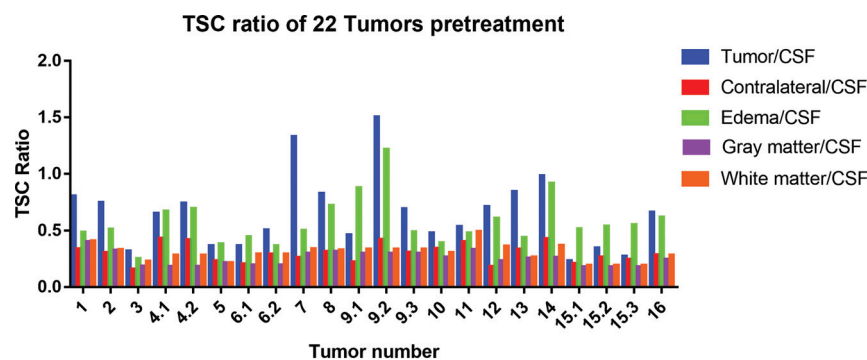


FIG 3. TSC ratio of 22 tumors pretreatment.

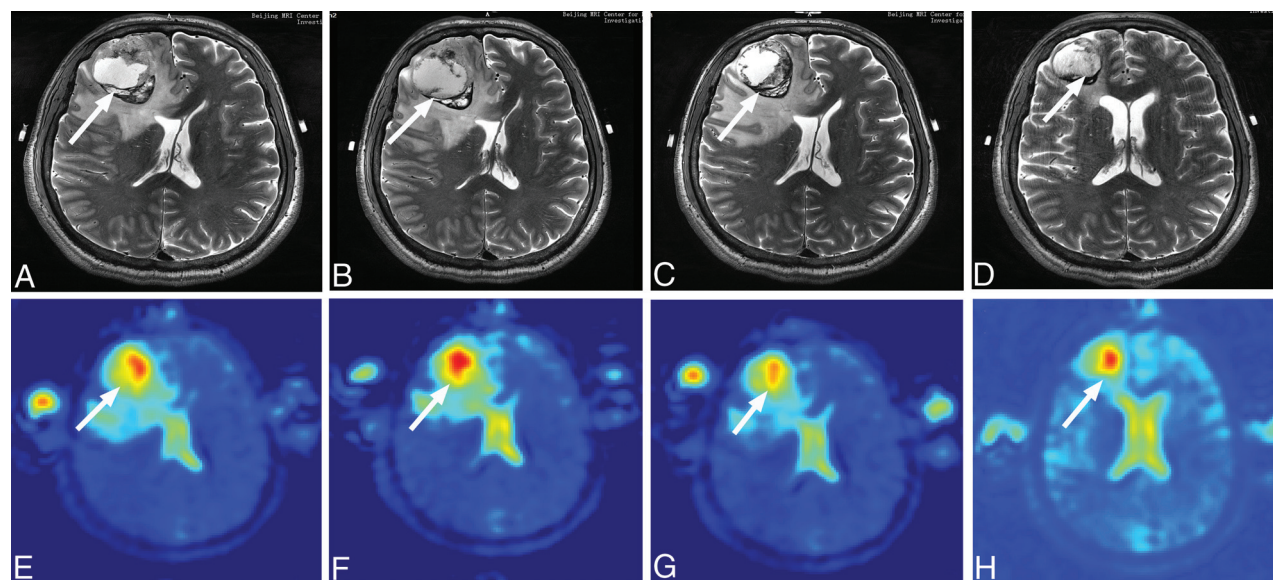


FIG 4. A, Axial T2-weighted image showing brain metastasis of pulmonary neuroendocrine carcinoma complicated with adenocarcinoma (tumor 14). B, T2-weighted image 48 hours after CK. C, T2-weighted image 1 week after CK. D, T2-weighted image 1 month after CK. E, Sodium MR imaging pretreatment. F, Sodium MR imaging 48 hours after CK. G, Sodium MR imaging 1 week after CK. H, Sodium MR imaging 1 month after CK. The arrows pointed to the metastasis.

main components: First, there is local production of factors that increase the tumor's vascular permeability, such as vascular endothelial growth factor (VEGF),³² glutamate,³³ and leukotriene.³⁴ Second, tumor vascular endothelial cells lack tight connections between them. The loss of blood-brain barrier integrity in brain tumors is largely attributable to the VEGF, the expression of which is also upregulated in gliomas, meningiomas, and metastatic tumors.³⁵⁻³⁸ VEGF expression has also been found to be significantly different in different pathologic types: VEGF expression in lung adenocarcinoma was observed to be significantly higher than that in squamous cell carcinoma.³⁹ The increased TSC values that we observed in the brain metastatic edema zones of lung adenocarcinoma also reflect the severity of the edema, which may be related to the actions of VEGF. This point needs to be confirmed by further research.

Our observed TSC values reflect the total amount of Na^+ inside and outside the cell, so the increased TSC values in tumors and edema zones may reflect this change in ion balance. In particular, a 60% increase in the Na^+ concentration in tumors requires a several-fold increase in intracellular Na^+ , a similar increase in the extracellular volume fraction, or a combination of both. The reason for this change is the decrease of Na^+/K^+ -ATPase enzyme activity and the change in Na/H exchange kinetics, which lead to the increase of intracellular Na^+ concentration and participate in malignant transformation of tumors. In this study, we only collected roughly descriptive statistics about the pathologic results of breast cancer brain metastases, lung cancer brain metastases, lymphomas, rectal cancer brain metastases, meningiomas, and liver cancer brain metastases. Among them, the Na^+ concentration in brain metastases of liver cancer was the highest, and that of breast cancer was the lowest. Biller et al⁶ showed that 7T sodium MRI can be used to help with the grading of gliomas in a study of 34 patients with World Health Organization grades I–IV untreated gliomas. Bartha et al⁷ characterized the metabolic profile of low-grade gliomas using short TE ^1H -MR spectroscopy and assessing the correlations between metabolite levels and sodium MR imaging. Although the Glu concentration is reduced and that of myo-inositol is elevated in low-grade glioma tissue, the $\text{NAA}/^{23}\text{Na}$ ratio was the most sensitive indicator of pathologic tissue. Biller et al⁶ found that the sodium signal was even superior to the molecular signature of *IDH* mutation status for progression prediction in gliomas. The information provided by sodium MR imaging may help to classify neoplasias at an early stage, reduce invasive tissue characterization procedures such as stereotactic biopsy specimens, and promote improved and individualized patient management in neuro-oncology by using imaging signatures of brain tumors. Future work should examine the potential for these metabolic parameters to distinguish among tumors of different pathologic types.

It is speculative to judge the prognosis of a tumor by the sodium concentration data before treatment. Multi-time quantitative observations could capture the changes of tumor sodium concentration in the early stage of SRT with CK more directly and help analyze the relationships between tumor TSC and internal environmental changes. In previous animal studies, only

sodium MR imaging was used to observe the changes of tumors after chemotherapy.⁴⁰ The imbalance of Na^+/K^+ -ATPase and ATP-dependent processes in cells can lead to ion imbalance, which, in turn, increases intracellular sodium. Because the ionic gradient can no longer be maintained, this issue can lead to cell death.⁴¹ According to Thulborn et al,⁸ these bioscales can monitor the spatial distribution of tissue responses to radiation treatment on at least a weekly basis. Such rapid feedback could be used to guide patient-adaptive radiation treatment and avoid excessive radiation administration when no response can be achieved.

The purpose of this study was to determine the change rule of TSC before any change in tumor volume occurs. Therefore, we assessed the volume and TSC of 12 lesions in 8 patients before treatment and 48 hours, 1 week, and 1 month after treatment and observed the overall change trends. The first TSC peak appeared within 48 hours after radiation therapy. Cell volume reduction and chromatin-condensed cells may have apoptotic characteristics,⁴¹ whereas sodium overload may be strongly related to apoptosis and even cause apoptosis itself. The first Na^+ concentration peak after CK SRT was caused by sodium overload after radiation, which, in turn, caused an increase in apoptosis, as reflected by the resulting destruction of cell membrane integrity. This result is consistent with our previous results of apoptosis imaging.⁴² The number of cells decreased at the later stage of apoptosis, and TSC subsequently decreased. These preliminary results suggest that sodium MR imaging provides reliable evidence in the early evaluation of the efficacy of radiation therapy for intracranial tumors. Tumors 7 and 14 showed a second TSC peak after 1 month, and those patients relapsed at 6 and 12 months after treatment, respectively. We speculate that this relapse was related to the active recurrence and proliferation of these tumors, increased cell division, resistance to radiation therapy, and vascular proliferation. These results illustrate that sodium MR imaging provides important supplementary information about biologic activity. It can be measured quantitatively and is noninvasive. Although sodium MR imaging is only used as a complementary method to proton MR imaging or other imaging methods such as PET, its great clinical value is still worthy of further study.

There are still several limitations of our study. The dual-tuned coil was not available, so B_0 shimming was completed with the proton coil, and the shimming parameters were transferred to sodium imaging. The change of coil resulted in the variation of the B_0 field, though we tried to keep the position of the patient consistent. It downgraded the performance of B_0 shimming and the SNR of sodium imaging. Other limitations of our study included the retrospective design, the small number of patients, and the relatively short follow-up period. More time points of follow-up and a larger sample are required to establish the long-term efficacy of sodium MR imaging. Improved software and technology are necessary to achieve accurate quantification of Na^+ concentrations because the current applications have many problems, and we will continue to study such improvements. Therefore, we must be cautious with our conclusions because the present findings are preliminary. Although a longer follow-up period and a larger sample are necessary to confirm these results, this study of

the evaluation of radiotherapeutic effects using sodium MR imaging for intracranial tumors had very encouraging results.

CONCLUSIONS

Changes in the TSC using sodium MR imaging can be used to detect radiobiologic alterations in brain tumors at early time points after CK radiation therapy. It can provide supplementary information to assist with individualized and accurate tumor treatment.

ACKNOWLEDGMENTS

The authors thank Fernando E. Boada from New York University for providing the twisted projection imaging sequence and tuning the scanning parameters.

Disclosure forms provided by the authors are available with the full text and PDF of this article at www.ajnr.org.

REFERENCES

- Adler JR, Murphy MJ, Chang SD, et al. **Image-guided robotic radiosurgery.** *Neurosurgery* 1999;44:1299–306; discussion 1306–07 [Medline](#)
- Witham TF, Okada H, Fellows W, et al. **The characterization of tumor apoptosis after experimental radiosurgery.** *Stereotact Funct Neurosurg* 2005;83:17–24 [CrossRef Medline](#)
- Tsuzuki T, Tsunoda S, Sakaki T, et al. **Tumor cell proliferation and apoptosis associated with the Gamma Knife effect.** *Stereotact Funct Neurosurg* 1996;66(Suppl 1):39–48 [CrossRef Medline](#)
- Kurita H, Ostertag CB, Baumer B, et al. **Early effects of PRS-irradiation for 9L gliosarcoma: characterization of interphase cell death.** *Minim Invasive Neurosurg* 2000;43:197–200 [CrossRef Medline](#)
- Haneder S, Giordano FA, Konstandin S, et al. **²³Na-MRI of recurrent glioblastoma multiforme after intraoperative radiotherapy: technical note.** *Neuroradiology* 2015;57:321–26 [CrossRef Medline](#)
- Biller A, Badde S, Nagel A, et al. **Improved brain tumor classification by sodium MR imaging: prediction of IDH mutation status and tumor progression.** *AJNR Am J Neuroradiol* 2016;37:66–73 [CrossRef Medline](#)
- Bartha R, Megyesi JF, Watling CJ. **Low-grade glioma: correlation of short echo time 1H-MR spectroscopy with ²³Na MR imaging.** *AJNR Am J Neuroradiol* 2008;29:464–70 [CrossRef Medline](#)
- Thulborn KR, Lu A, Atkinson IC, et al. **Quantitative sodium MR imaging and sodium bioscales for the management of brain tumors.** *Neuroimaging Clin N Am* 2009;19:615–24 [CrossRef Medline](#)
- Ouwerkerk R, Bleich KB, Gillen JS, et al. **Tissue sodium concentration in human brain tumors as measured with ²³Na MR imaging.** *Radiology* 2003;227:529–37 [CrossRef Medline](#)
- Laymon CM, Oborski MJ, Lee VK, et al. **Combined imaging biomarkers for therapy evaluation in glioblastoma multiforme: correlating sodium MRI and F-18 FLT PET on a voxel-wise basis.** *Magn Reson Imaging* 2012;30:1268–78 [CrossRef Medline](#)
- Baskar R, Lee KA, Yeo R, et al. **Cancer and radiation therapy: current advances and future directions.** *Int J Med Sci* 2012;9:193–99 [CrossRef Medline](#)
- Schepkin VD, Bejarano FC, Morgan T, et al. **In vivo magnetic resonance imaging of sodium and diffusion in rat glioma at 21.1 T.** *Magn Reson Med* 2012;67:1159–66 [CrossRef Medline](#)
- Nagy I, Lustyik G, Lukács G, et al. **Correlation of malignancy with the intracellular Na⁺:K⁺ ratio in human thyroid tumors.** *Cancer Res* 1983;43:5395–402 [Medline](#)
- Ng KH, Bradley DA, Looi LM. **Elevated trace element concentrations in malignant breast tissues.** *Br J Radiol* 1997;70:375–82 [CrossRef Medline](#)
- Rose AM, Valdes R. **Understanding the sodium pump and its relevance to disease.** *Clin Chem* 1994;40:1674–85 [Medline](#)
- Madelin G, Kline R, Walvick R, et al. **A method for estimating intracellular sodium concentration and extracellular volume fraction in brain in vivo using sodium magnetic resonance imaging.** *Sci Rep* 2014;4:4763 [CrossRef Medline](#)
- Hilal SK, Maudsley AA, Simon HE, et al. **In vivo NMR imaging of tissue sodium in the intact cat before and after acute cerebral stroke.** *AJNR Am J Neuroradiol* 1983;4:245–49 [Medline](#)
- Jones SC, Kharlamov A, Yanovski B, et al. **Stroke onset time using sodium MRI in rat focal cerebral ischemia.** *Stroke* 2006;37:883–88 [CrossRef Medline](#)
- Maarouf A, Audoin B, Konstandin S, et al. **Topography of brain sodium accumulation in progressive multiple sclerosis.** *Magn Reson Mater Phy* 2014;27:53–62 [CrossRef Medline](#)
- Reetz K, Romanzetti S, Dogan I, et al. **Increased brain tissue sodium concentration in Huntington's disease: a sodium imaging study at 4 T.** *Neuroimage* 2012;63:517–24 [CrossRef Medline](#)
- Schepkin VD, Chenevert TL, Kuszpit K, et al. **Sodium and proton diffusion MRI as biomarkers for early therapeutic response in subcutaneous tumors.** *Magn Reson Imaging* 2006;24:273–78 [CrossRef Medline](#)
- Huang L, Zhang Z, Qu B, et al. **Imaging of sodium MRI for therapy evaluation of brain metastases with CyberKnife at 7T: a case report.** *Cureus* 2018;10:e2502 [CrossRef Medline](#)
- Lu A, Atkinson IC, Claiborne TC, et al. **Quantitative sodium imaging with a flexible twisted projection pulse sequence.** *Magn Reson Med* 2010;63:1583–93 [CrossRef Medline](#)
- O'Donnell M, Edelstein WA. **NMR imaging in the presence of magnetic field inhomogeneities and gradient field nonlinearities.** *Med Phys* 1985;12:20–06 [CrossRef Medline](#)
- Kothari RU, Brott T, Broderick JP, et al. **The ABCs of measuring intracerebral hemorrhage volumes.** *Stroke* 1996;27:1304–05 [CrossRef Medline](#)
- Spector M, O'Neal S, Racker E. **Phosphorylation of the beta subunit of Na⁺:K⁺-ATPase in Ehrlich ascites tumor by a membrane-bound protein kinase.** *J Biol Chem* 1980;255:8370–73 [CrossRef Medline](#)
- Cameron IL, Smith NK, Pool TB, et al. **Intracellular concentration of sodium and other elements as related to mitogenesis and oncogenesis in vivo.** *Cancer Res* 1980;40:1493–50 [Medline](#)
- Weidner N. **Tumor angiogenesis: review of current applications in tumor prognostication.** *Semin Diagn Pathol* 1993;10:302–13 [Medline](#)
- Summers RM, Joseph PM, Kundel HL. **Sodium nuclear magnetic resonance imaging of neuroblastoma in the nude mouse.** *Invest Radiol* 1991;26:233–41 [CrossRef Medline](#)
- Thulborn KR, Davis D, Adams H, et al. **Quantitative tissue sodium concentration mapping of the growth of focal cerebral tumors with sodium magnetic resonance imaging.** *Magn Reson Med* 1999;41:351–59 [CrossRef Medline](#)
- Hashimoto T, Ikehira H, Fukuda H, et al. **In vivo sodium-23 MRI in brain tumors: evaluation of preliminary clinical experience.** *Am J Physiol Imaging* 1991;6:74–80 [Medline](#)
- Senger DR, Brown LF, Claffey KP, et al. **Vascular permeability factor, tumor angiogenesis and stroma generation.** *Invasion Metastasis* 1994;14:385–94 [Medline](#)
- Baethmann A, Maier-Hauff K, Schürer L, et al. **Release of glutamate and of free fatty acids in vasogenic brain edema.** *J Neurosurg* 1989;70:578–91 [CrossRef Medline](#)
- Black KL, Hoff JT, McGillicuddy JE, et al. **Increased leukotriene C4 and vasogenic edema surrounding brain tumors in humans.** *Ann Neurol* 1986;19:592–95 [CrossRef Medline](#)
- Carlson MR, Pope WB, Horvath S, et al. **Relationship between survival and edema in malignant gliomas: role of vascular endothelial growth factor and neuronal pentraxin 2.** *Clin Cancer Res* 2007;13:2592–98 [CrossRef Medline](#)

36. Provias J, Claffey K, delAguila L, et al. **Meningiomas: role of vascular endothelial growth factor/vascular permeability factor in angiogenesis and peritumoral edema.** *Neurosurgery* 1997;40:1016–26 [CrossRef Medline](#)
37. Strugar JG, Criscuolo GR, Rothbart D, et al. **Vascular endothelial growth/permeability factor expression in human glioma specimens: correlation with vasogenic brain edema and tumor-associated cysts.** *J Neurosurg* 1995;83:682–89 [CrossRef Medline](#)
38. Yano S, Shinohara H, Herbst RS, et al. **Expression of vascular endothelial growth factor is necessary but not sufficient for production and growth of brain metastasis.** *Cancer Res* 2000;60:4959–67 [Medline](#)
39. Zebrowski BK, Yano S, Liu W, et al. **Vascular endothelial growth factor levels and induction of permeability in malignant pleural effusions.** *Clin Cancer Res* 1999;5:3364–68 [Medline](#)
40. Schepkin VD, Ross BD, Chenevert TL, et al. **Sodium magnetic resonance imaging of chemotherapeutic response in a rat glioma.** *Magn Reson Med* 2005;53:85–92 [CrossRef Medline](#)
41. Boada FE, LaVerde G, Jungreis C, et al. **Loss of cell ion homeostasis and cell viability in the brain: what sodium MRI can tell us.** *Curr Top Dev Biol* 2005;70:77–101 [CrossRef Medline](#)
42. Sun L, Zhou K, Wang W, et al. **[18F]ML-10 imaging for assessment of apoptosis response of intracranial tumor early after radiosurgery by PET/CT.** *Contrast Media Mol Imaging* 2018;2018:1–9 [CrossRef Medline](#)